

# Journal Club- Critical Appraisal

- Topic: **Amide proton transfer imaging of adult diffuse gliomas: correlation with histopathological grades**
- Date: 18.05.2020
- Presenters: Dr Foo, Dr Thoo, Dr Hayati M
- Lecturer: In-Charge Dr Nur Asma Sapiai

# I- Overview of the paper

- Publishing journal and the year
- Article title
- Authors and their institutions

# Neuro-Oncology

*Neuro-Oncology* 16(3), 441–448, 2014  
doi:10.1093/neuonc/not158  
Advance Access date 4 December 2013

- Publishing Journal, Scopus, MEDLINE, EMBASE Indexed
- Year of Publication

## Amide proton transfer imaging of adult diffuse gliomas: correlation with histopathological grades

- Title: clearly mentioned
- Authors, Institutions

**Osamu Togao, Takashi Yoshiura, Jochen Keupp, Akio Hiwatashi, Koji Yamashita, Kazufumi Kikuchi, Yuriko Suzuki, Satoshi O. Suzuki, Toru Iwaki, Nobuhiro Hata, Masahiro Mizoguchi, Koji Yoshimoto, Koji Sagiyama, Masaya Takahashi, and Hiroshi Honda**

*Department of Molecular Imaging and Diagnosis, Graduate School of Medical Science, Kyushu University, Fukuoka, Japan (O.T.); Department of Clinical Radiology, Graduate School of Medical Science, Kyushu University, Fukuoka, Japan (O.T., T.Y., A.H., K.Y., K.K., H.H.); Philips Research, Hamburg, Germany (J.K.); Philips Electronics Japan, Tokyo, Japan (Y.S.); Department of Neuropathology, Graduate School of Medical Sciences, Kyushu University, Fukuoka, Japan (S.O.S., T.I.); Department of Neurosurgery, Graduate School of Medical Sciences, Kyushu University, Fukuoka, Japan (N.H., M.M., K.Y.); Advanced Imaging Research Center, UT Southwestern Medical Center, Dallas, Texas (K.S., M.T.)*

**Corresponding author:** Osamu Togao, MD, PhD, Department of Molecular Imaging and Diagnosis, Graduate School of Medical Science, Kyushu University, Fukuoka, Japan; 3-1-1 Maidashi Higashi-ku Fukuoka, 812-8582 Japan (togao@radiol.med.kyushu-u.ac.jp).

# II- Abstract

- Aim: mentioned clearly

**Background.** Amide proton transfer (APT) imaging is a novel molecular MRI technique to detect endogenous mobile proteins and peptides through chemical exchange saturation transfer. We prospectively assessed the usefulness of APT imaging in predicting the histological grade of adult diffuse gliomas.

**Methods.** Thirty-six consecutive patients with histopathologically proven diffuse glioma (48.1 ± 14.7 y old, 16 males and 20 females) were included in the study. APT MRI was conducted on a 3T clinical scanner and was obtained with 2 s saturation at 25 saturation frequency offsets  $\omega = -6$  to  $+6$  ppm (step 0.5 ppm).  $\delta B_0$  maps were acquired separately for a point-by-point  $\delta B_0$  correction. APT signal intensity (SI) was defined as magnetization transfer asymmetry at 3.5 ppm: magnetization transfer ratio  $(MTR)_{asym} = (S_{[-3.5 \text{ ppm}]} - S_{[+3.5 \text{ ppm}]})/S_0$ . Regions of interest were carefully placed by 2 neuroradiologists in solid parts within brain tumors. The APT SI was compared with World Health Organization grade, Ki-67 labeling index (LI), and cell density.

**Methods:** Did not clearly explained the study design. Confusing statement: HPE first or APT first?  
Mentioned about study group, sample size, gender, age, and procedure rendered to each group and measuring tool

## II- Abstract

**Results:** The measured variables with their statistical analysis and significance.

**Results.** The mean APT SI values were  $2.1 \pm 0.4\%$  in grade II gliomas ( $n = 8$ ),  $3.2 \pm 0.9\%$  in grade III gliomas ( $n = 10$ ), and  $4.1 \pm 1.0\%$  in grade IV gliomas ( $n = 18$ ). Significant differences in APT intensity were observed between grades II and III ( $P < .05$ ) and grades III and IV ( $P < .05$ ), as well as between grades II and IV ( $P < .001$ ). There were positive correlations between APT SI and Ki-67 LI ( $P = .01$ ,  $R = 0.43$ ) and between APT SI and cell density ( $P < .05$ ,  $R = 0.38$ ). The gliomas with microscopic necrosis showed higher APT SI than those without necrosis ( $P < .001$ ).

**Conclusions.** APT imaging can predict the histopathological grades of adult diffuse gliomas.

**Conclusion:** clearly answer the question of interest.

# III- Rationale of study

- Diagnosis of gliomas relies on the **HPE** as a gold standard, as well as molecular profile and genetic information.
- MRI – noninvasive. Contributes to: the management decisions in all phases of diagnosis, treatment, and follow-up of patients with gliomas.



# III- Rationale of study

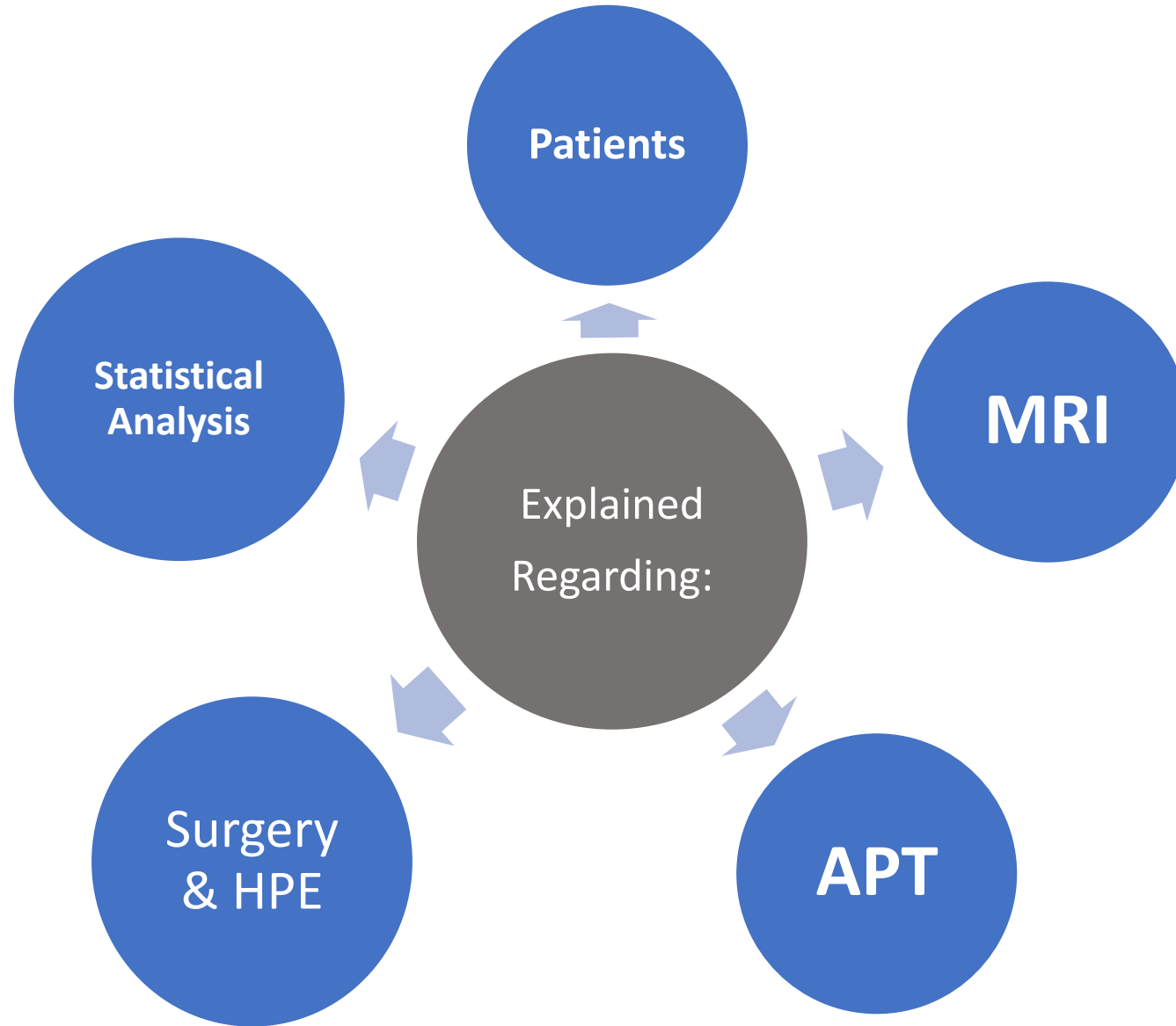
- Basic MRI sequences are **still not accurate**- can underestimate/ overestimate grading.
- Previous studies on DWI, PWI, MRS on grading glioma: some contradicting.
- **Therefore it is desirable to develop a novel imaging method that complements other MR methods and thus improves accuracy in grading gliomas.**
  - **Well and clearly written.**
  - **References to earlier works.**
  - **expressed the importance and limitations of what is previously acknowledged**

# Objective:

- To prospectively assess the ability of APT imaging for predicting the grade of adult diffuse gliomas with histopathological evaluations.
- **Clearly mentioned**



Methodology: Explained in 5 different sections



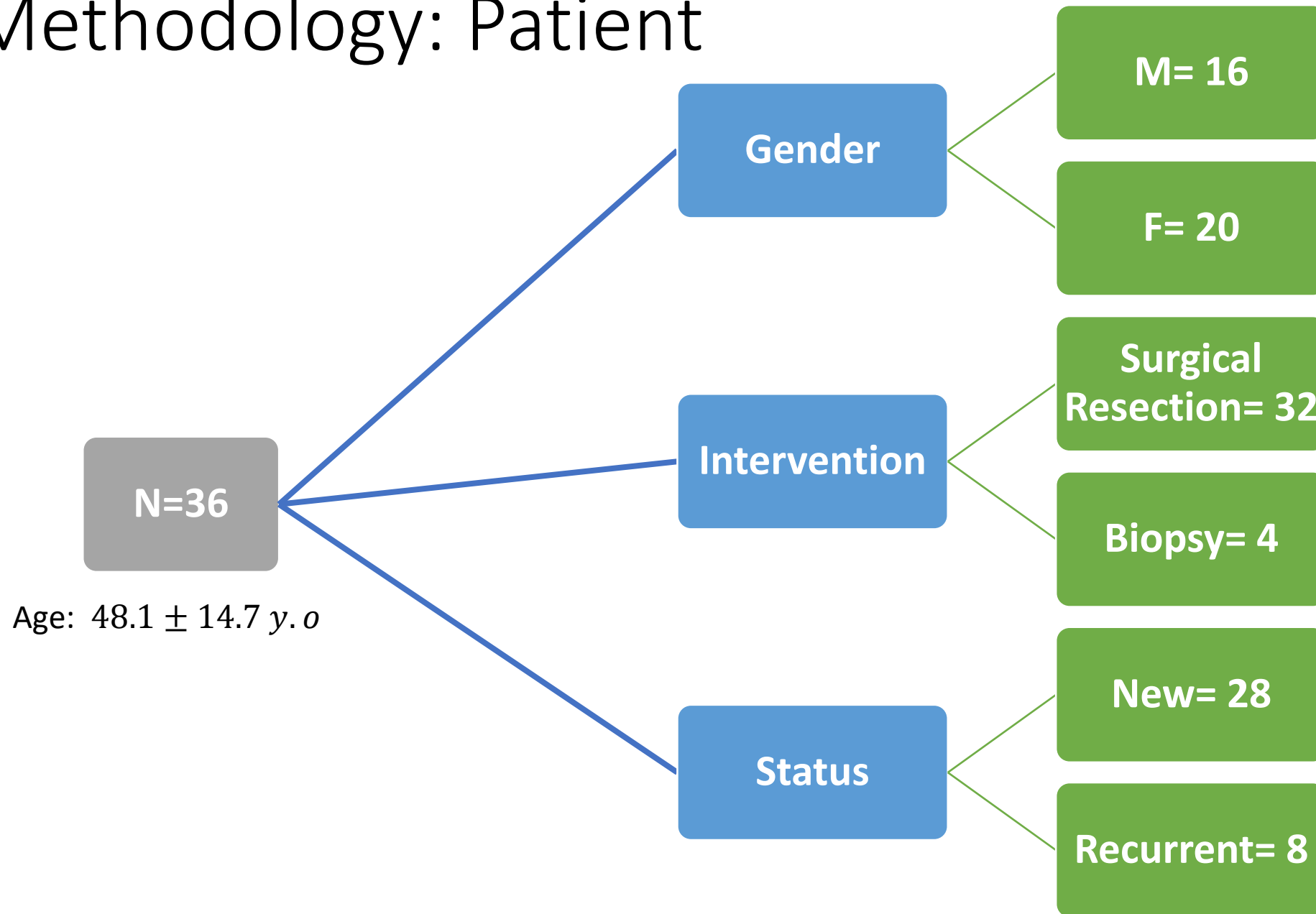
# Materials and Methods

## *Patients*

Thirty-six consecutive adult patients with diffuse glioma ( $48.1 \pm 14.7$  y old, 16 males and 20 females) who underwent subsequent surgical resection ( $n = 32$ ) or biopsy ( $n = 4$ ) were included in this prospective study. Recurrent

- Study design: Prospective study – mentioned
- Study population: 36 patients with diffuse gliomas, but did not mention selection based on MRI (with APT)?
- Study duration: Not mentioned. But did mention interval between MRI and surgery was  $< 2$  weeks in all patients
- Study area: Not mentioned

# Methodology: Patient



- Inclusion criteria & exclusion criteria: not mentioned.
- No randomization process.
- Approved by institutional review board, informed consent taken.

# Methodology: MRI

Described in great detail regarding MRI machine, coils, acquisition, sequences TR/TE

## MRI

MRI was performed on a 3T clinical scanner (Achieva TX, Philips Healthcare) equipped with a second-order shim, using an 8-channel head coil for signal reception and 2-channel parallel transmission via the body coil for radiofrequency (RF) transmission. The acquisition software was modified to alternate the operation of the 2 transmission channels during the RF saturation pulse, which enables long quasi-continuous RF saturation beyond the 50% duty cycle of a single RF amplifier, and to allow a special RF shimming for the saturation homogeneity of the alternated pulse.<sup>21</sup>

On a single slice corresponding to a maximum cross-section area of a tumor, 2-dimensional (2D) APT imaging was performed using a saturation pulse with a duration of 2 s (40 × 50 ms, sinc-gauss-shaped elements) and a saturation power level corresponding to  $B_{1,rms} = 2 \mu\text{T}$ . For acquiring an APT Z-spectrum, the imaging was repeated at 25 saturation frequency offsets from  $\omega = -6$  to +6 ppm with a step of 0.5 ppm as well as 1 far off-resonant frequency ( $\omega = -160$  ppm) for signal normalization.

The other imaging parameters were as follows: fast spin-echo readout with driven equilibrium refocusing; echo train length (ETL) 128 (single-shot fast spin-echo); sensitivity encoding (SENSE) factor 2; repetition time (TR) = 5000 ms; echo time (TE) = 6 ms; Matrix = 128 × 128 (reconstructed to 256 × 256); slice thickness = 5 mm, field of view = 230 × 230 mm; scan time = 2 min 20 s for one Z-spectrum. A  $\Delta B_0$  map for off-resonance correction was acquired separately using a 2D gradient echo with identical spatial resolution, and it was used for a point-by-point  $\Delta B_0$  correction.

For reference, several standard MRIs, including T1-weighted, T2-weighted, FLAIR, and contrast enhanced T1-weighted images, were acquired. The following parameters were used—T2-weighted: ETL = 8, TR/TE = 3000/80 ms, 18 slices, thickness = 5 mm, SENSE factor = 1.6; T1-weighted: 3D magnetization-prepared rapid-segmented gradient-echo sequence, TR/TE = 2000/20 ms, inversion time = 800 ms, 18 slices, thickness = 1 mm, SENSE factor = 1.6; FLAIR: ETL = 27, TR/TE/2800 ms, 18 slices, SENSE factor = 1.6. The APT images were acquired before the administration of the gadolinium contrast agent in all patients.

# Methodology: MRI

- 3T clinical MRI scanner (Achieva TX, Philips Healthcare)
- For reference, standard MRI sequences acquired: T1W, T2W, FLAIR, Post contrast T1W
- APT was acquired before gadolinium administration.

# Methodology: APT

## APT Imaging Data Analysis

All image data were analyzed with the software program ImageJ v1.43u (National Institutes of Health [NIH]). A plug-in was created to assess the Z-spectra and magnetization transfer ratio asymmetry ( $MTR_{asym}$ ) equipped with a correction function for  $B_0$  inhomogeneity, using interpolation among the Z-spectral image data. First, rigid body motion correction was performed using the TurboReg algorithm.<sup>22</sup> The local  $B_0$  field shift, in hertz, was obtained from the  $B_0$  map, which was created from dual-echo gradient-echo images ( $TE = 1$  and  $2$  ms) according to the following equation:  $\Delta B_0(x) = (\text{Phase}[TE_2](x) - \text{Phase}[TE_1](x)) / (TE_2 - TE_1) * 2 * \pi$ , where  $\text{Phase}[TE_i](x)$  indicates phases of the images with echo times  $TE_1$  or  $TE_2$  at position  $x$  in radians, and  $TE_1$  and  $TE_2$  are given in seconds. The  $\Delta B_0(x)$  is the resulting  $B_0$  map measured in hertz. Each voxel was corrected in image intensity for the nominal saturation frequency offset by Lagrange interpolation among the neighboring Z-spectral images. This procedure corresponds to a frequency shift along the saturation frequency offset axis according to the measured  $B_0$  shift.

The MTR was defined as  $1 - S_{sat}/S_0$ , where  $S_{sat}$  and  $S_0$  are the SIs obtained with and without selective saturation, respectively.<sup>17</sup> To reduce these undesired contributions from conventional magnetization transfer (MT) effect and direct saturation of bulk water, an asymmetry analysis of

MTR with respect to the water frequency was performed. For APT imaging, the asymmetry analysis at 3.5 ppm downfield from the water signal was calculated as  $MTR_{asym}(3.5 \text{ ppm})$ :

$$\begin{aligned} MTR_{asym}(3.5 \text{ ppm}) &= \frac{S_{sat}(-3.5 \text{ ppm}) - S_{sat}(+3.5 \text{ ppm})}{S_0} \\ &= MTR'_{asym}(3.5 \text{ ppm}) + APTR \end{aligned}$$

where  $MTR'_{asym}$  is the inherent asymmetry of the conventional MT effect, and APTR is the amide proton transfer ratio.<sup>17</sup> Thus, it should be noted that the measured  $MTR_{asym}(3.5 \text{ ppm})$  is an apparent APT signal and thus it is appropriate to define the calculated  $MTR_{asym}(3.5 \text{ ppm})$  images as APT weighted. In the present study, APT SI was defined as  $MTR_{asym}(3.5 \text{ ppm}) \times 100$  (%). The normalized APT SI was also calculated as the difference in APT SI between tumor and normal-appearing white matter (NAWM).

Described in great detail regarding APT physics equations

# APT imaging Data Analysis

- In the quantitative analysis:
- APT SIs were independently evaluated by 2 experienced neuroradiologists (14 and 12 y, respectively, of experience in neuroradiology)
- - who were blinded to the clinical and histopathological data.
- 4 circular ROIs ( $\sim 0.3 \text{ cm}^2$ , 36pixels) were carefully placed by each observer in the solid component of a tumor to include the area with the highest APT signal determined with visual inspection.
- Area of cystic, large necrotic, or hemorrhagic components of the tumor were avoided with reference to conventional MRI.
- The strategy for the ROI analysis was based on the concept that regions of a tumor demonstrating the greatest grade determine the histological grade of the tumor. The measured APT signals in 4 ROIs were averaged to represent the tumor. The APT signal was also measured in a larger circular ROI ( $\sim 1.8 \text{ cm}^2$ , 200pixels) placed in NAWM .



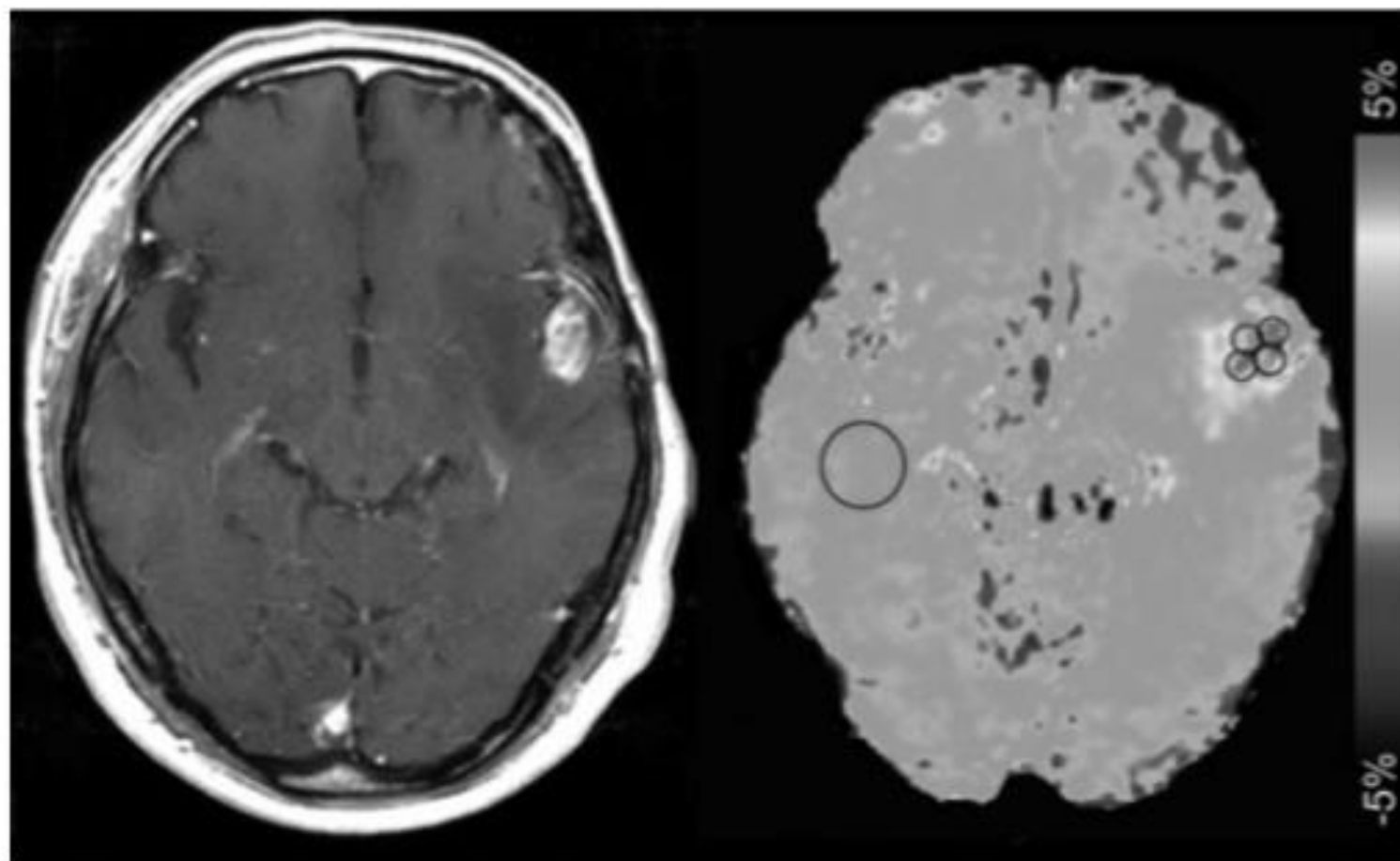


**Fig. 1.** Placement of ROIs. Four circular ROIs were carefully placed in the solid component of a tumor to include the area with the highest APT signal determined by visual inspection. Cystic, necrotic, or hemorrhagic components were avoided with reference to conventional MRI. An ROI was also placed in contralateral NAWM.

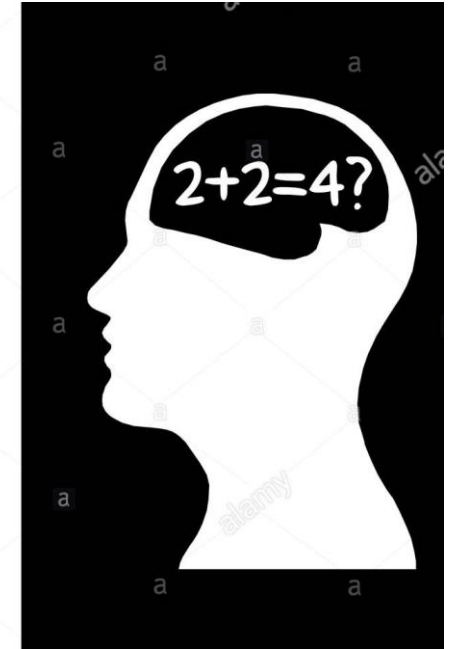
- In this study, all image data were analyzed with the software program ImageJ v1.43u (National Institutes of Health [NIH])

# Surgical and pathological evaluation

- HPE from the surgical resections- diagnosis is based on WHO criteria by established neuropathologies.
- Described about Ki-67 labelling index (LI) and determination of the percentage of positively labelled cells.
- Described about cell density measurement

# Overall statistical analysis

- Descriptive values: mean and SD
- Interobserver agreement for the tumour APT SI by the 2 neuroradiologists
  - simple linear regression
  - intraclass correlation coefficient (ICC)



Interrater, test-retest, and intrarater reliability of numerical/continuous →  
Excellent if  $>0.74$   
*Agreed well.*

- Hence, APT SI for every patients were averaged
- APT SI → compared among different groups of gliomas (grade II-IV) – ANOVA (compare means more than two independent variable), followed by Tukey's Multiple comparison test
- APT SI → Ki-67 or cell density: simple linear regression (relationships between two continuous (quantitative) variables).
- APT SI → were compared between gliomas with and without intratumoral necrosis by Student's t-Test.
- Statistical analyses : IPSS , IBM 19.
- P value was given (if  $< 0.05$  = statistically significant).

# Result:

Togao et al.: Amide proton transfer imaging for grading diffuse glioma

**Table 1.** APT SI, normalized APT SI, and Ki-67 LI in each WHO grade and histology

Histology	Number	APT SI (%)		Normalized APT SI (%)		Ki-67 LI	
Grade II (n = 8)							
Astrocytoma	4	2.2 ± 0.3	2.1 ± 0.4	2.1 ± 0.2	1.8 ± 0.7	6.0 ± 4.7	7.2 ± 5.6
Oligodendroglioma	3	1.8 ± 0.4		1.3 ± 0.9		5.2 ± 3.4	
Oligoastrocytoma	1	2.5		2.3		17.8	
Grade III (n = 10)							
Anaplastic astrocytoma	3	3.6 ± 1.3	3.2 ± 0.9*	2.7 ± 2.1	2.9 ± 1.6	16.5 ± 9.9	14.6 ± 7.5
Anaplastic oligodendroglioma	5	3.2 ± 0.6		3.2 ± 0.9		15.0 ± 6.2	
Anaplastic oligoastrocytoma	2	2.5 ± 0.3		2.3 ± 0.7		14.0 ± 2.8	
Grade IV (n = 18)							
Glioblastoma multiforme	18	4.1 ± 1.0***, +		3.8 ± 1.2**		35.3 ± 19.2***, ++	

\* $P < .05$ , \*\* $P < .01$ , \*\*\* $P < .001$ , compared with grade II.

+ $P < .05$ , ++ $P < .01$ , compared with grade III.

**Mean APT SI in Grade III and IV were >> Grade II gliomas ( $p < 0.0001$ )**

**High grade glioma high APT SI with higher Ki-67**

# Interobserver agreement

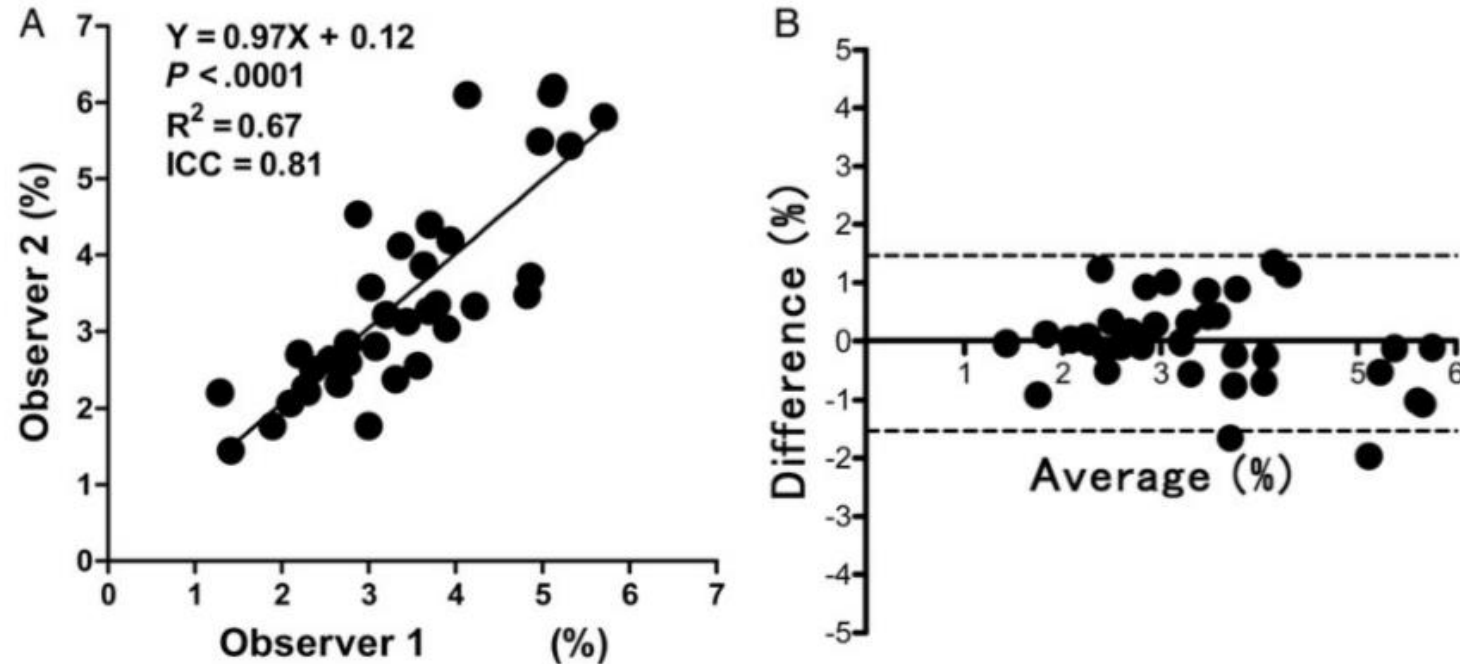


**Fig. 2.** Analyses of interobserver agreement. (A) The linear regression analysis shows high correlation in the APT SIs measured by the 2 observers. (B) The Bland–Altman analysis of the APT SIs measured by the 2 observers shows high concordance. Dashed lines show 95% limits of agreement.

**Excellent interobserver agreement, ICC 0.81, B&A=concordance**

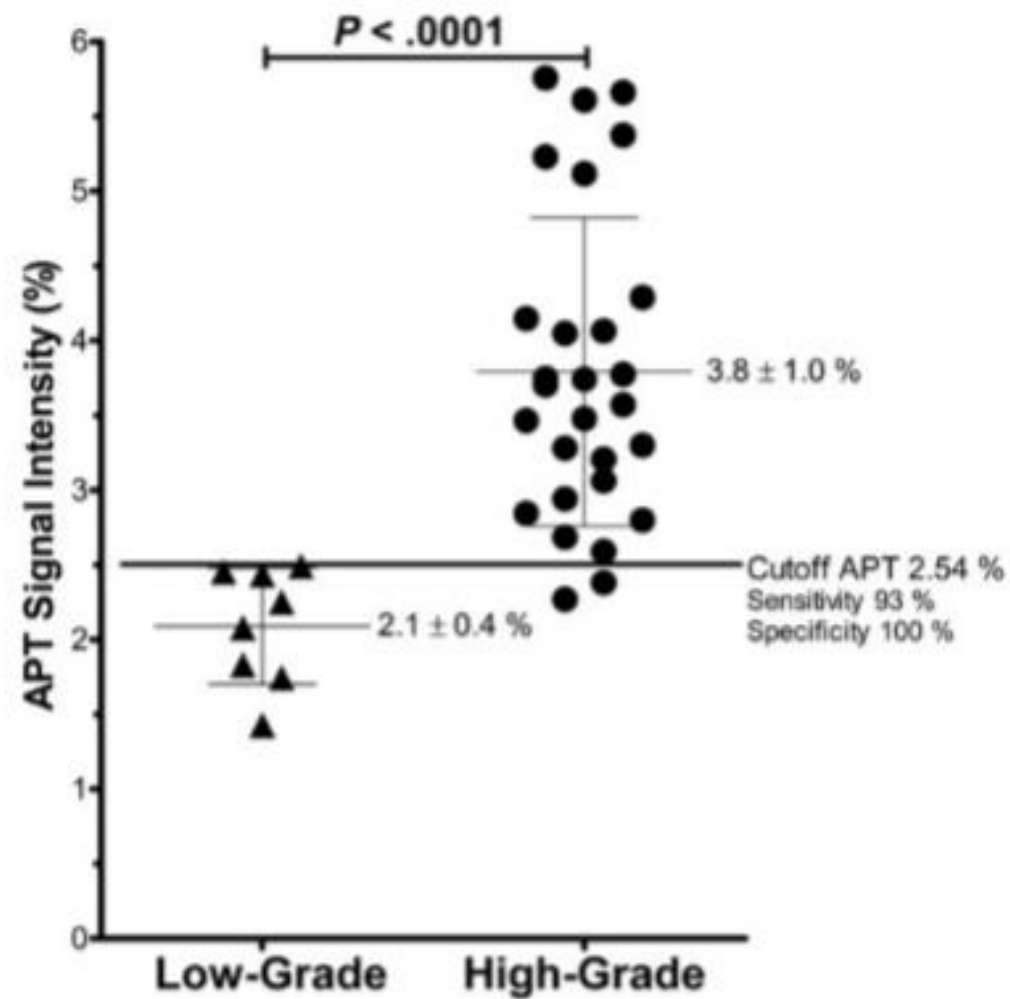
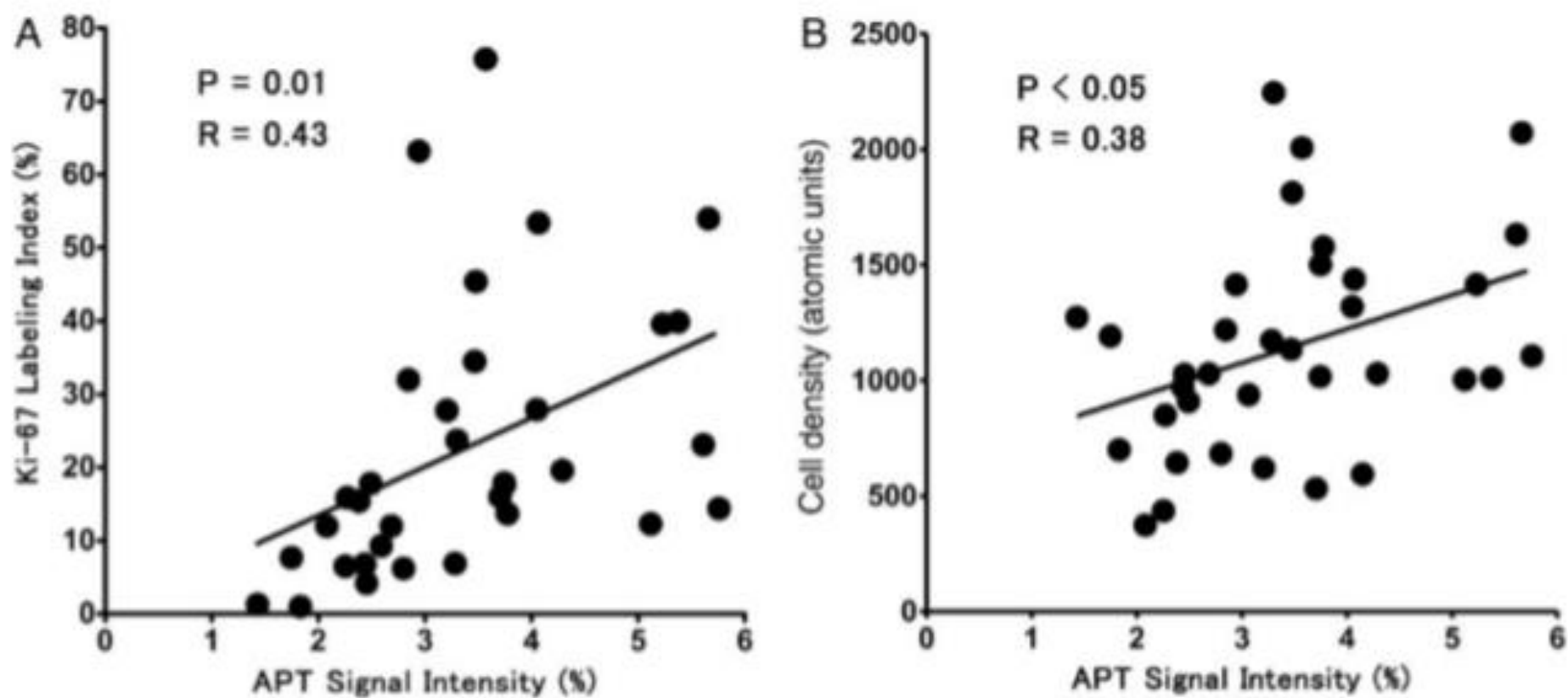


**Fig. 3.** APT SI in low-grade (grade II) and high-grade (grades III and IV) glioma. The APT SIs in the high-grade gliomas were higher than in the low-grade glioma.





**g. 4.** Correlation between APT SI and Ki-67 LI (A) or cell density (B). Moderate positive correlations are noted between the parameters.

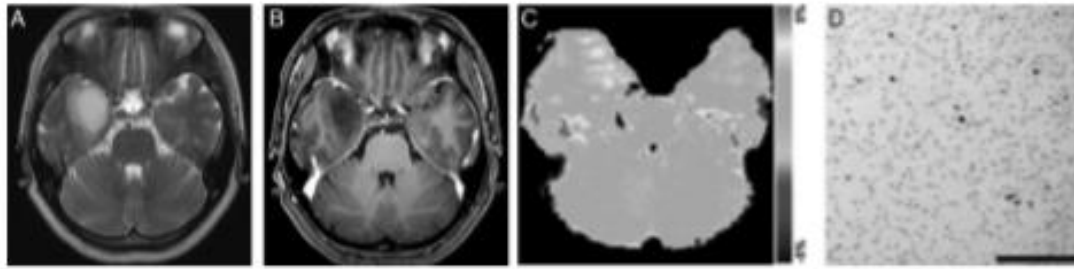


**Fig. 5.** Astrocytoma (grade II) in a 42-year-old woman. (A) A transverse T2-weighted MRI shows a homogeneous hyperintensity area in the right temporal lobe. (B) A contrast enhanced transverse T1-weighted image shows no enhancement in the tumor. (C) The APT-weighted image shows a mild increase in SI (APT SI, 1.4%) in the tumor compared with normal brain tissue. (D) Ki-67 immunohistochemical staining shows few positive cells, indicating low proliferative activity of the tumor (Ki-67 LI, 1.3%).

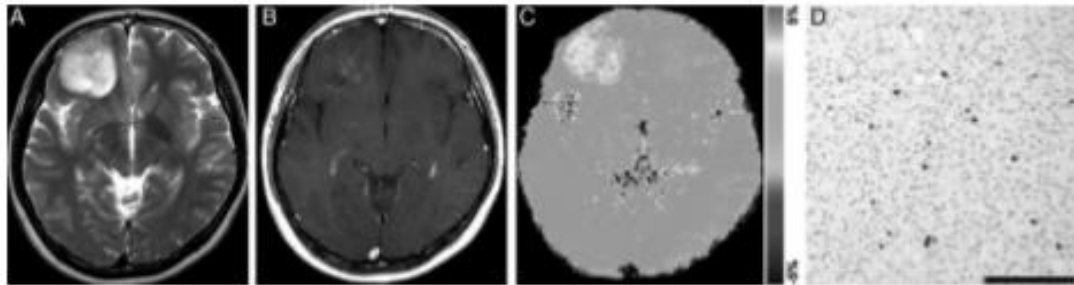


**Fig. 6.** Anaplastic oligodendroglioma (grade III) in a 25-year-old woman. (A) A transverse T2-weighted image shows a rather heterogeneously hyperintense area in the right frontal lobe. (B) A contrast enhanced transverse T1-weighted image shows faint enhancement in the tumor. (C) The APT-weighted image shows a mild to moderate increase in SI (APT SI, 2.8%) in the tumor compared with normal brain tissue. (D) Ki-67 immunohistochemical staining shows scattered positive cells (Ki-67 LI, 6.2%).

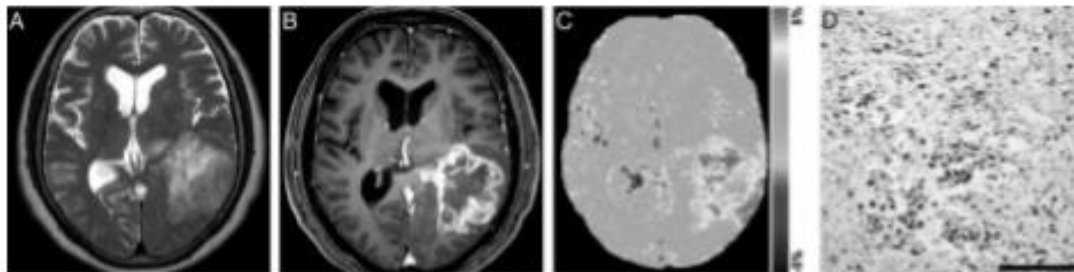


**Fig. 7.** Glioblastoma multiforme (grade IV) in a 70-year-old woman. (A) A transverse T2-weighted image shows a heterogeneously hyperintense area in the left temporal lobe. (B) A contrast enhanced transverse T1-weighted image shows heterogeneous ringlike enhancement in the tumor. (C) The APT-weighted image shows high SI in the tumor compared with normal brain tissue (APT SI, 4.0%). (D) Ki-67 immunohistochemical staining shows a large number of positive cells, indicating high proliferative activity of the tumor (Ki-67 LI, 27.9%). High cell density is also noted.

Image: Correlation with standard MRI sequences, APT and HPE (Ki-67 and cell density)

# Statistical significance

- Appropriate tests for data
- Confidence interval and P value were given, 95% and  $<0.05$  respectively.
- Clearly mentioned the main findings (APT SI, normalized APT SI, Ki-67).
- Mentioned the clinical significance of the result.

(glioblastoma multiforme), respectively. Higher APT SI was observed in the higher-grade gliomas. The increase in APT SI was accompanied by an elevation of Ki-67 LI, which suggested more active proliferation of tumor cells in the higher-grade gliomas.

# Confounding factors

- Did not mention about **important potential confounders**
- Inclusion criteria / exclusion criteria not stated

## Funding:

- This work supported by the Japanese Society of Neuroradiology, Japanese Radiological Society, Philips Electronics Japan, and Bayer Healthcare, Japan
- Conflict of interest: 2 of the authors are from Philips

# Limitations

1) **Difficulty in accordance of location** for the ROIs of the APT measurements with the areas for Ki 67 and cell density.

- Resected specimens possess little locational information.

2) **single-slice acquisition** used in the APT sequence due to limitation of total acquisition time in patient scans. Protocols with a fast 3D coverage are desirable for future studies in order to better characterize the typical tumor tissue heterogeneity in all dimensions.

3) ROIs placed in the solid component by manually visual inspection. Some contributions of **microcysts** that were invisible on images, and extracellular fluid might affect the result.

4) Number of low-grade gliomas Grade II) was small compared with that of high-grade gliomas.

# Limitations:

Rapidly developing fields, the imaging protocols have not yet fully optimized especially in human studies.

## **In our setting**

- Relatively new in HUSM (only few cases done in 2020).
- Many radiographers, MMeds, Radiologists are not familiar with APT

# Suggestions:

- With the knowledge of APT as a predictive tool for glioma grading, we can apply to our HUSM setting– similar MRI Philips 3T, software is available
- Training by Philips app specialist to conduct APT study among radiographers
- Training for MMed and Radiologist for interpretation of APT for better outcome for patients.
- Later, can widen the scope of APT usage, not only for glioma detection/grading but for other indications (e.g ischemia, haemorrhage etc).

# Overall:

- It is a good article. Supported by other similar articles.

## **Strength:**

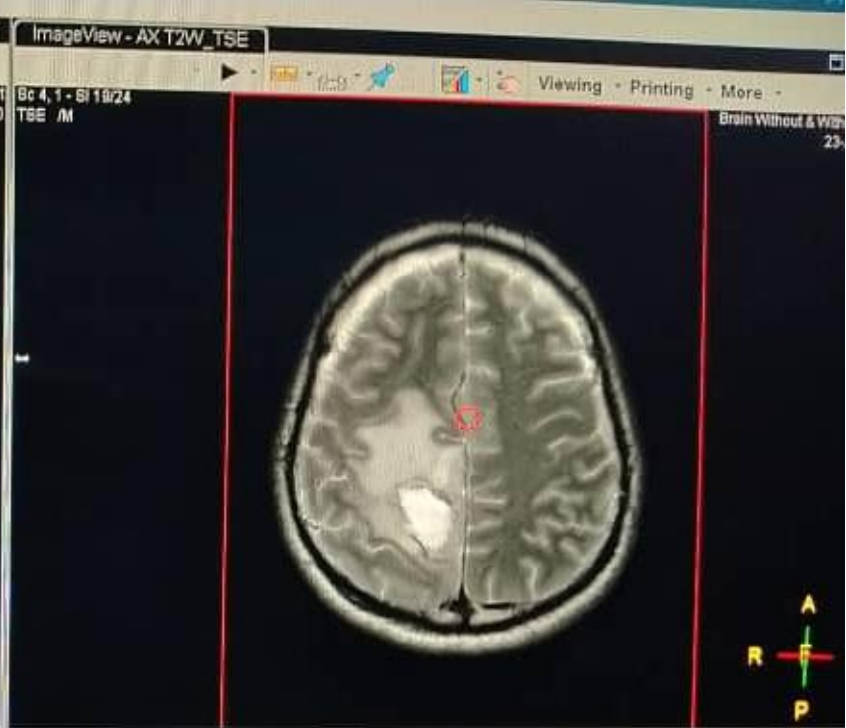
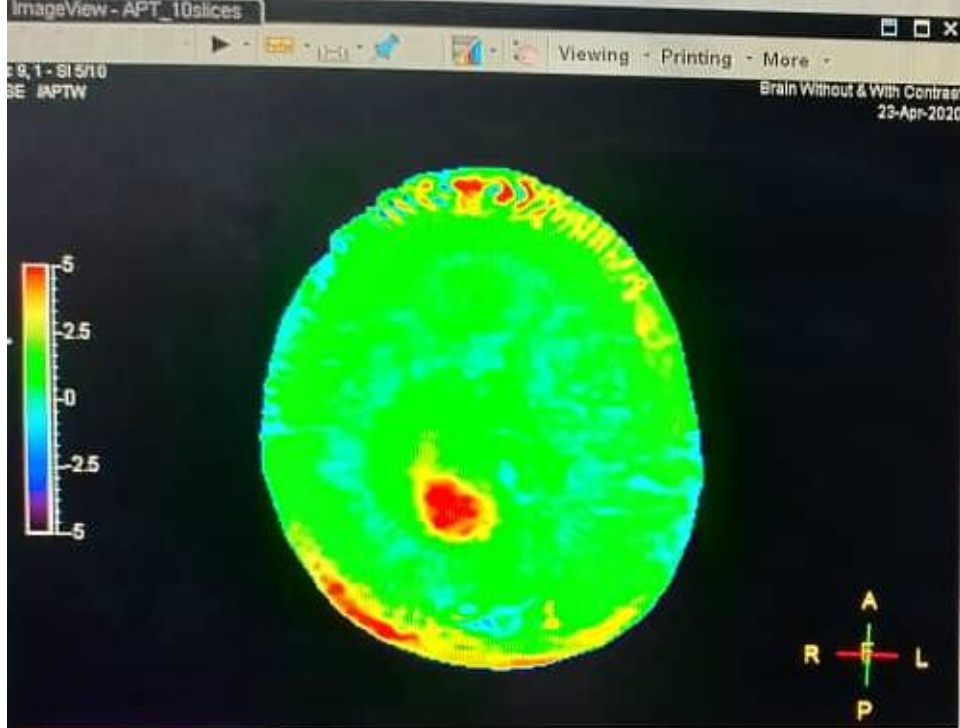
- Prospective design
- Short duration interval between imaging and surgery (<2weeks)
- Complete histo-pathology diagnosis in all patients



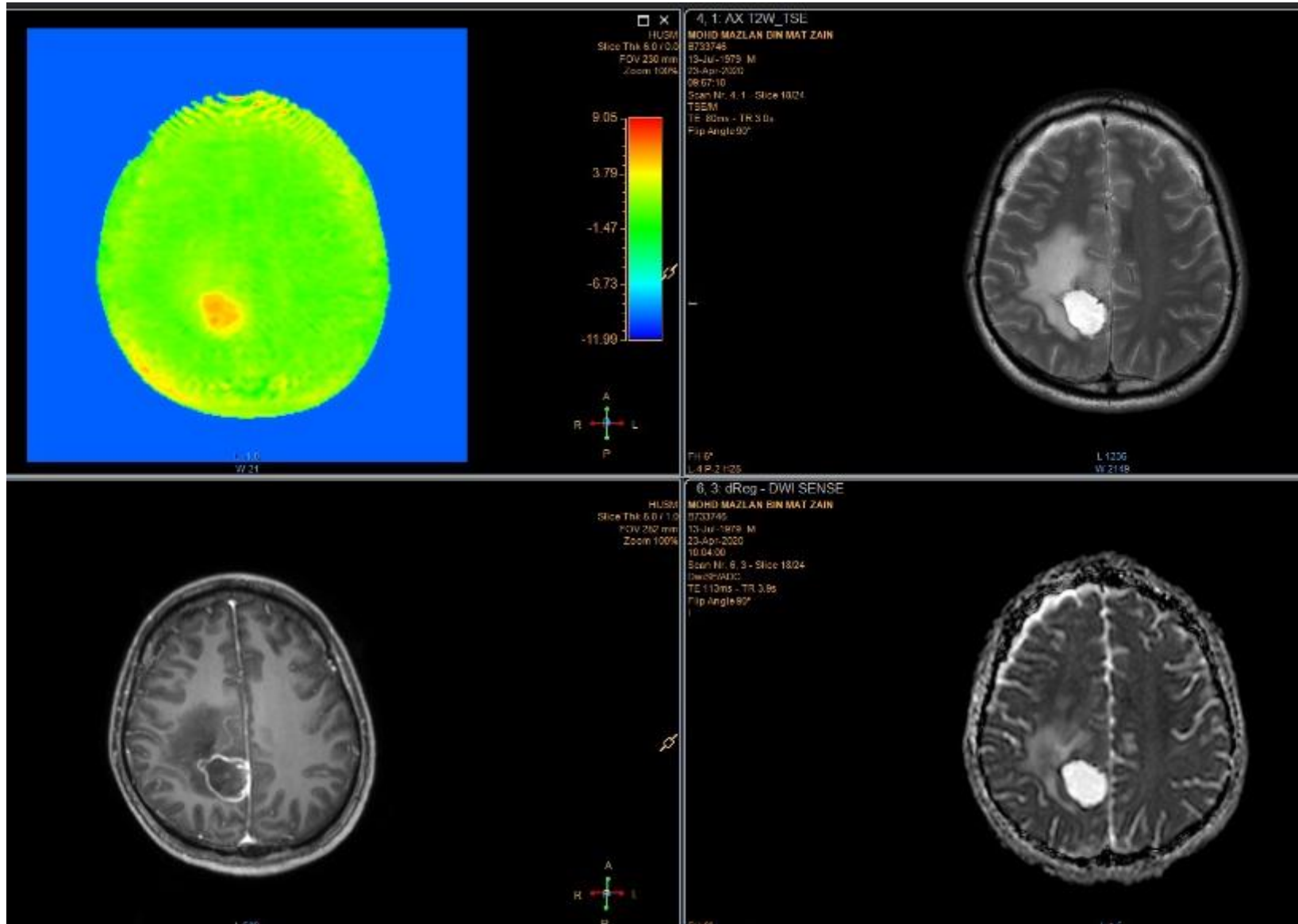
# References:

- Al-Jundi, A., & Sakka, S. (2017). Critical Appraisal of Clinical Research. *Journal of clinical and diagnostic research : JCDR*, 11(5), JE01–JE05. <https://doi.org/10.7860/JCDR/2017/26047.9942>

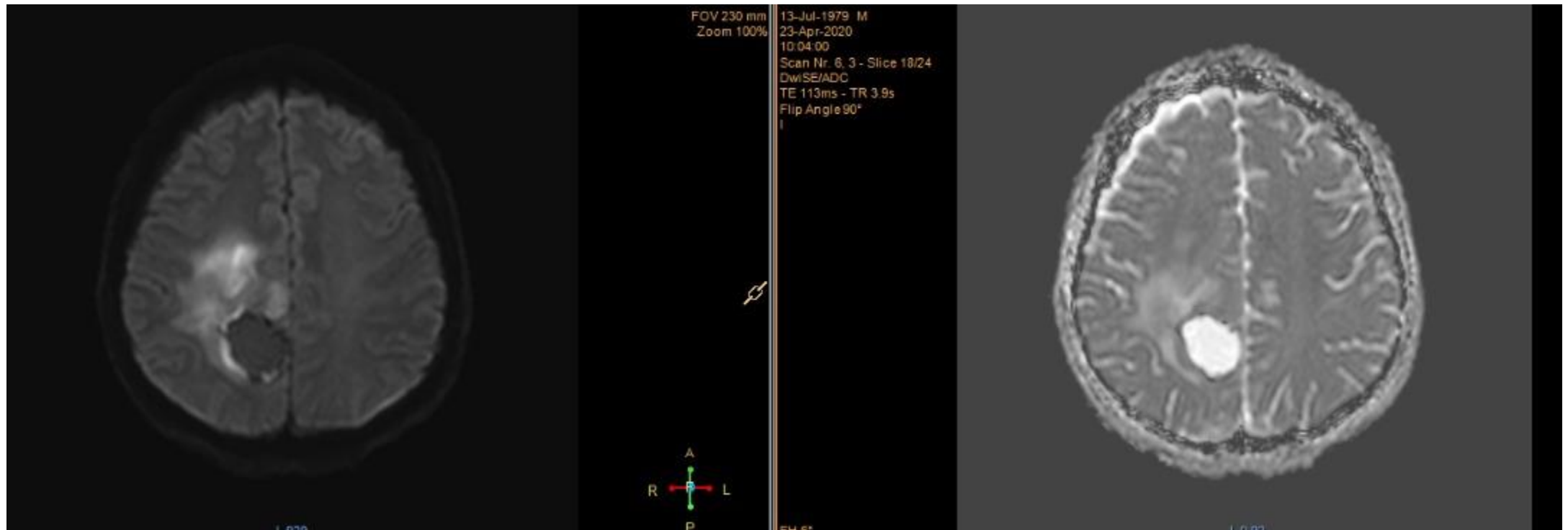
Example of case in our setting



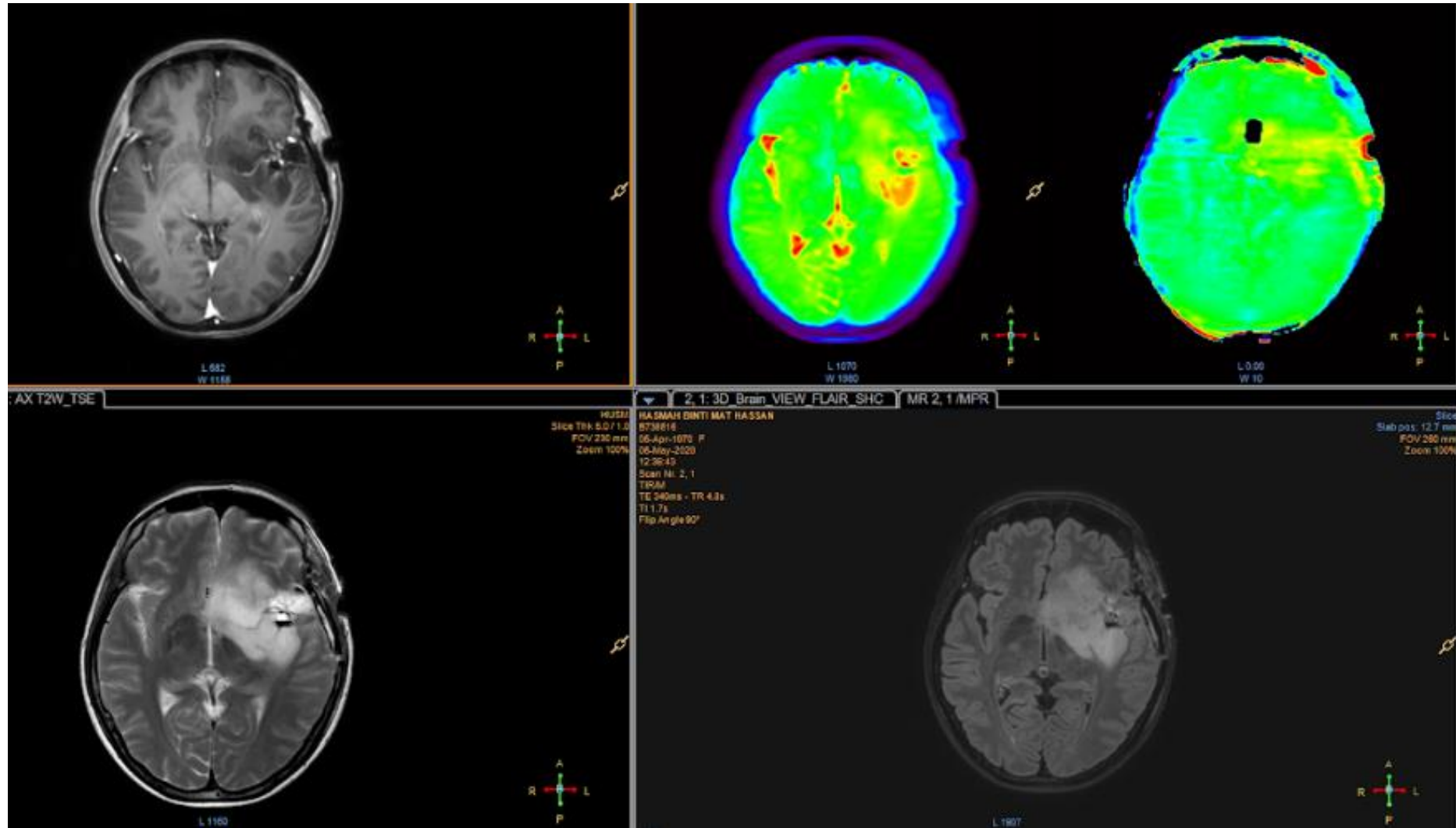
# Patient 1



- DWI



# Patient 2



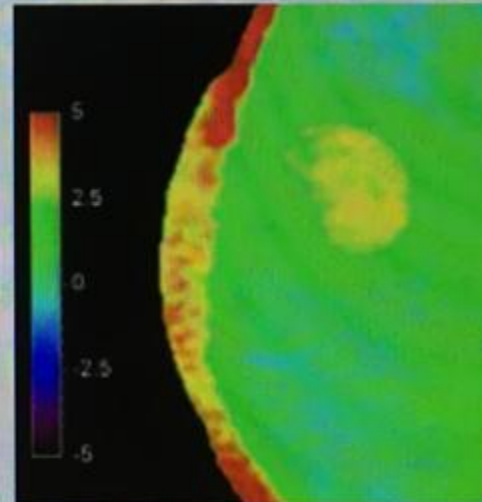
- We have to use IPS workstation for qualitatively interpret APT, not appearing in PACS.

## Voxel-by-voxel analysis

2. The asymmetry of the Z-spectrum is evaluated by subtracting the positive frequency side from the negative side and normalized to an unsaturated image  $S_0$ .  $MTR_{asym}(\%) = (S_{-\Delta\omega} - S_{\Delta\omega}) / S_0$

The resulting  $MTR_{asym}$  value at +3.5 ppm is displayed as percent level (relative to  $S_0$ ) in the final APT<sub>w</sub> images, and referred to as APT<sub>w</sub>%.  $APT_w\% = MTR_{asym}[\Delta\omega = +3.5\text{ppm}](\%)$

The display shows a range from green (0% APT<sub>w</sub>%) to red (5% APT<sub>w</sub>%).



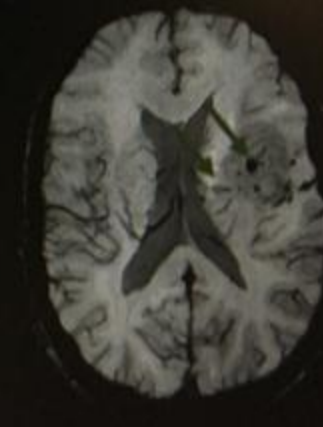
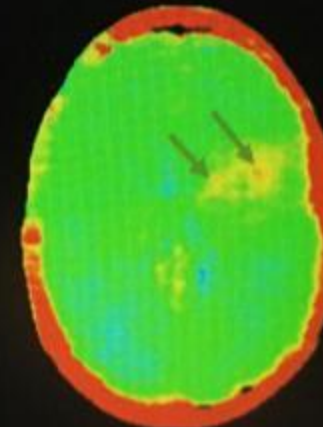
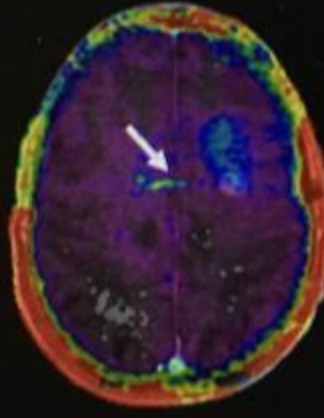
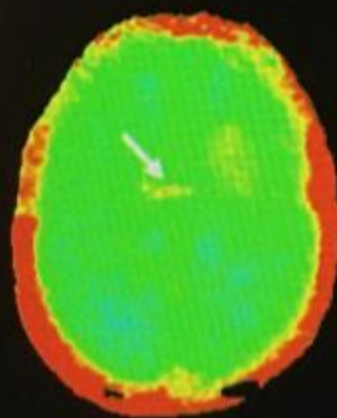


# Confounders

Not all red areas are high-grade glioma.

- Some confounders can also be red (high MTR<sub>asym</sub>).
- Confounders should be assessed with alternate imaging techniques.

Confounder	Technique
Fat	Fat suppression: <u>mDIXON</u> , SPIR, SPAIR
Cyst	FLAIR, T2w
Blood vessel	<u>SWIp</u> , MRA
Blood products	<u>SWIp</u> , T2 FFE
Non-glioma tumor	Department tumor protocol



## Using 3D APT

For tumor grading on the APT<sub>w</sub> images:

- Normal white matter and gray matter appear green.
- Hyper intensities (yellow and red) may indicate solid tissue areas of grade III and IV tumor.
- The highest tumor grade found in sub-regions of the lesion is the determinant for the overall grade.

Adhere 3D APT to routine radiology procedures for diagnosis. Use APT to assist with tumor grading.